On the Orientational Mobility of Water Molecules in Proton and Sodium Terminated Nafion Membranes

W. Ensing,[†] J. Hunger,[†,‡] N. Ottosson,[*,†] and H.J. Bakker[†]

FOM Institute AMOLF, Science Park 104, 1098 XG Amsterdam, The Netherlands

E-mail: ottosson@amolf.nl

[*]To whom correspondence should be addressed

[†]FOM Institute AMOLF, Science Park 104, 1098 XG Amsterdam, The Netherlands

[‡]Present: Molecular Spectroscopy Department, Max Planck Institute for Polymer Research, Ackermannweg 10, 55128 Mainz, Germany

Abstract

We study the dielectric properties of proton and sodium terminated Nafion at varying degrees of hydration with a frequency-domain coaxial-line reflectometric method (1.5 – 20 GHz) and with time-domain THz-pulse spectroscopy (0.7 – 1.5 THz). The water content is varied from 1 to 12 water molecules per Nafion polymer unit. At low hydration levels, we observe that the orientational mobility of the water molecules embedded in the Nafion membrane channels is strongly slowed down in comparison to bulk water. Only at the highest hydration level the rotational mobility of the water molecules becomes similar to that of bulk water. We also observe that the mobilities of protons and sodium ions strongly depend on the degree of hydration of the Nafion membranes and that the mobility of the proton is more strongly decreased than that of sodium upon lowering the hydration level.

Keywords: Water, Protons, Sodium Ions, Nafion, GHz reflectrometry, THz spectroscopy

Introduction

Proton transport in aqueous media is anomalously fast compared to that of other ions[1]. This anomaly is a consequence of the fact that protons are transported by structural diffusion, also known as the Grotthuss mechanism, whereas most other ions are transported by mass diffusion. In 1995, Noam Agmon proposed a mechanistic model of proton transfer in bulk liquid water that involves a sequence of Eigen-Zundel-Eigen transitions, triggered by hydrogen bond cleavage in the proton's second hydration shell[2]. This mechanism is based on the interconversion of a hydrogen bond and a covalent bond, allowing a proton to shuttle from an initial Eigen complex ($H_9O_4^+$) via an intermediate Zundel complex ($H_5O_2^+$) to another Eigen complex located at another position in the liquid[3,4]. The interconversion of hydration structures is accompanied by the flow of an electron in the opposite direction. Proton transfer in water therefore primarily involves transferring the charge of the proton, not its mass. In this process, water reorientation is thought to be the

rate limiting process. Measuring the reorientation time of the water molecules therefore can give information on the mobility of protons.

Protons dissolved in water are often found in a confined state: in lipid bilayers[5], membrane proteins[6], ion channels[6], and/or in the vicinity of other ions. The transfer of protons in nanoporous aqueous media also plays a crucial role in the generation and storage of energy in biological systems and in industrial electrochemical systems, such as the proton exchange membrane (PEM) fuel cells. In this article we study the behavior of protons in the nano-channels of Nafion membranes, which constitute the most widely used proton exchange membranes in PEM fuel cells.

Nafion is a sulfonated tetrafluoroethelyne (Teflon)-based fluoropolymer (Figure 1A). Its hydrophobic Teflon backbone (the red part) provides mechanical strength to the Nafion membrane, while its hydrophilic sulfonated perfluorovinyl ether side chains (the blue part) allow for the formation of nano-scale hydrophilic domains[7–10] (Figure 1B).

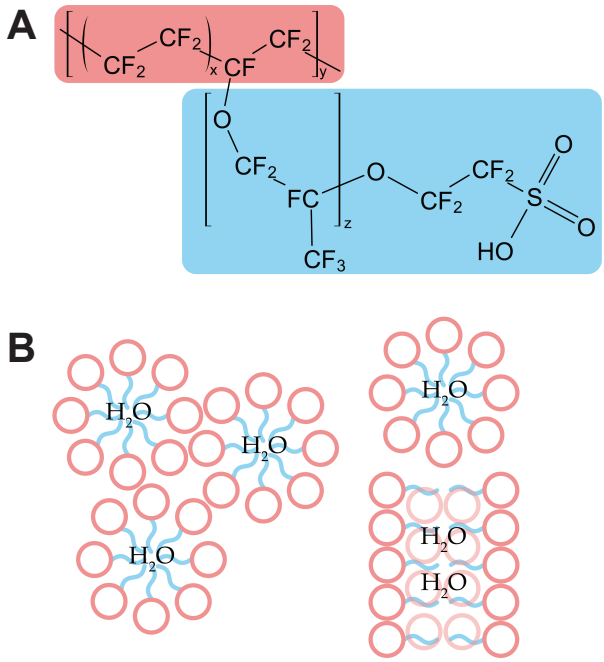

Figure 1: (A) Chemical structure of Nafion and (B) a schematic representation of hydrophilic domains in Nafion. Blue features indicate hydrophilic parts of the Nafion polymer units, red features indicate hydrophobic parts.

The selective hydration of the side-chains[11], the dependence of the conductivity on the hy-

dration level[12], the proton dissociation mechanism of the Nafion side chains[13], and many other features of Nafion have been studied extensively. The proton conductivity of Nafion has been successfully modeled as an interplay of Grotthuss conduction, mass transport, and surface conductivity[14].

Here we experimentally explore the properties of Nafion membranes containing protons or sodium ions using GHz-THz dielectric relaxation spectroscopy. This technique allows us to directly probe the dielectric relaxation of the dipoles of water molecules. The strength and the frequency dependence of this relaxation give information on the number of rotational mobile water molecules and the extent of their rotational mobility. Using this technique, we can also extract the conductivity of sodium terminated and protonated Nafion membranes at different degrees of hydration.

Experiment

We measure dielectric spectra, $\hat{\varepsilon}(\omega)$, at GHz-THz frequencies. The real part represents the in-phase polarization of the sample and the imaginary part the loss (dissipation) in the sample. The total permittivity is given by:

$$\hat{\varepsilon}(\omega) = \varepsilon'(\omega) - i\varepsilon''(\omega) \tag{1}$$

At GHz frequencies the response of neat water at room temperature is dominated by a loss peak in $\varepsilon''(\omega)$ at 20 GHz and a corresponding dispersion in $\varepsilon'(\omega)$. This response is due to the rotation of the dipolar water molecules. Additionally, an Ohmic loss term, $i\frac{\sigma}{\omega\varepsilon_0}$, is measured for conductive samples with conductivity σ (ε_0 is the vacuum permittivity). Therefore, measuring the complex permittivity gives us information on both the rotational mobility of water molecules and the conductivity of protons and sodium ions in the Nafion membranes.

To reliably extract the orientational relaxation of water, frequencies ranging from the GHz to the THz range have to be studied. This broad frequency range cannot be covered in a single

experiment. In the GHz range we use a frequency-domain coaxial-line reflectometric method to cover a frequency range of 1.5–20 GHz. In the range of 0.7–1.5 THz we measure the sample's complex permittivity by means of time-domain THz-pulse spectroscopy. A detailed description of the experiment can be found in the Supporting Material.

Nafion Samples

The Nafion was purchased as 0.180 mm thick membranes in the proton-terminated form. For the GHz measurements, the membranes were cut into circles with a diameter of 9.0 mm. After removing all organic impurities by washing the samples in 3% H_2O_2 at 50 °C for 24 hours, half the membranes were treated with 1 M HCl at 50 °C for 24 hours to ensure that the sulfonate end-groups of all side chains of the Nafion were protonated. The other half of the membranes was treated with 1 M NaOH at 50 °C for 24 hours to replace all protons at the sulfonate end-groups of the side chains of the Nafion with sodium ions, i.e. to prepare the Nafion in the sodium terminated form. After this treatment the Nafion membranes were rinsed with ultra-pure water and dried in a vacuum chamber for 24 hours. The membranes were placed in desiccators containing P_2O_5, saturated salt solutions or pure water to obtain a range of relative humidities (RH): P_2O_5 was used for 5% RH, K_2CO_3 for 44% RH, NaCl for 75.4% RH, and pure water for 99% RH[15]. The membranes were kept in desiccators for at least one week, for it has been shown that the water uptake of Nafion can take several days[16]. The membranes were kept in the desiccators until they were stacked in the measurement jacket and on the probe head (see Supporting Material). To ensure the removal of air and excess water between the membranes, mechanical pressure was applied during the measurements.

For the THz-measurements, the Nafion membranes were cut into $\sim$2 cm radius half-circles that fitted into the cavities of the spacer of the sample holder. After cleaning, terminating with H^+ or Na^+ ions, and drying, they were kept in a desiccator with a home-built humidity controller for 5 hours at 5%, 50%, and 99% relative humidity. The membranes were transferred to the cuvette just before the measurement, so that the humidity of the Nafion membranes was well defined during

the measurement.

The water content of the Nafion samples was determined by weighing the GHz-samples after one week in the desiccators ($m_{sample,wet}$) and after drying for 24 hours in a vacuum chamber ($m_{sample,dry}$). Using the molecular weight of the Nafion polymer units[17], M_{Nafion} = 1100 g/mol, and the molecular weight of water molecules, M_{water} = 18.02 g/mol, the number of water molecules per Nafion polymer unit is calculated, λ_{tot}. The mass of the Nafion is taken to be equal to the mass of the dry sample, $m_{Nafion} = m_{sample,dry}$, and the mass of the water is taken to be the difference in mass between the dry and the wet sample, i.e. $m_{water} = m_{sample,wet} - m_{sample,dry}$. The water content, λ_{tot} is calculated as

$$\lambda_{tot} = \frac{m_{water}}{M_{water}} \cdot \frac{M_{Nafion}}{m_{Nafion}} \, . \tag{2}$$

λ_{tot} is determined for all humidities for both sodium terminated Nafion and protonated Nafion. The results are denoted in Table 1. The obtained water contents are in excellent agreement with previous measurements[16].

Results and Discussion

We have fitted the observed dielectric response of both the sodium and proton phase Nafion samples to various relaxation models. The very broad relaxation behavior observed in Figs. 2 and 3 makes the use of individual Debye relaxation modes unsuitable, unless a large number of closely spaced modes would be invoked. Therefore we model the total response as a sum of a single Cole-Cole relaxation mode and a conductivity term.

$$\hat{\varepsilon}(\omega) = \frac{S_1}{1 + (i\omega\tau)^{(1-\alpha)}} - i\frac{\sigma}{\omega\varepsilon_0} + \varepsilon_\infty \tag{3}$$

Here, S_1 gives the strength of the Cole-Cole mode, τ is the typical reorientation time of the water dipoles, σ is the conductivity, and ε_∞ is the permittivity that can be considered constant in the

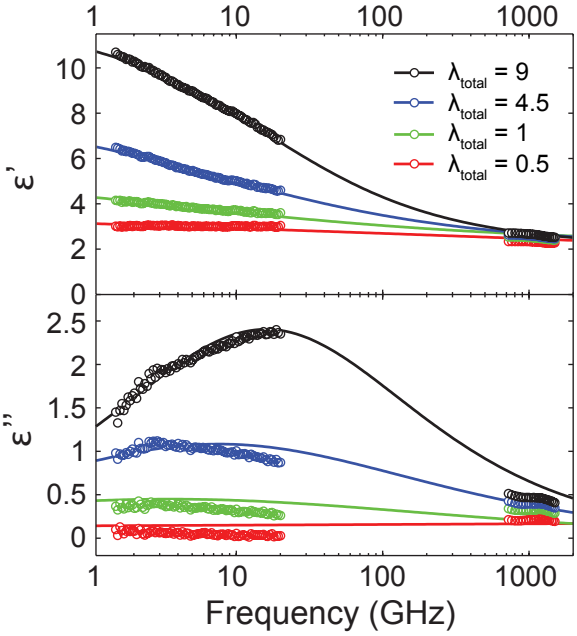

Figure 2: Permittivity of sodium terminated Nafion in the GHz and THz frequency range, as a function of $\nu = \frac{\omega}{2\pi}$. The measured permittivity is shown as open circles. The fit is shown as solid lines. The conductivity term has been subtracted.

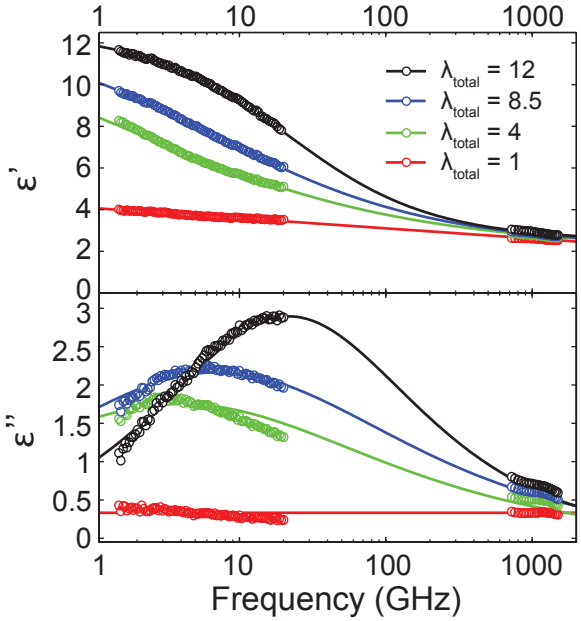

Figure 3: Permittivity of protonated Nafion in the GHz and THz frequency range, as a function of $\nu = \frac{\omega}{2\pi}$. The measured permittivity is shown as open circles, the fit is shown as solid lines. The conductivity term has been subtracted.

frequency range of the orientational polarization, resulting from high frequency polarization contributions (i.e. intra- and intermolecular vibrations, electronic, nuclear). The Cole-Cole parameter, α, represents the width of the time-constant distribution. For $\alpha = 0$, the Cole-Cole distribution becomes identical to that of Debye relaxation in which all water molecules have the same reorientation time, τ. For $\alpha = 1$, all reorientation times are equally present, i.e. the complex permittivity becomes $\hat{\varepsilon}(\omega) = \frac{S_1}{2} - i\frac{\sigma}{\omega\varepsilon_0} + \varepsilon_\infty$.

The conductivity σ, which for aqueous electrolyte systems can be considered constant in the frequency range here considered[28], can be determined accurately from the low-frequency dielectric response (since it goes as $i\frac{\sigma}{\omega\varepsilon_0}$); around 1 GHz the dielectic response of both sodium terminated and protonated Nafion is dominated by Ohmic loss. To visually better resolve the contribution of the water orientational response to the imaginary part we have subtracted the conductivity term from the data shown for sodium terminated Nafion in Figure 2 and for protonated Nafion in Figure 3 – the corresponding raw data and decomposition into relaxation and conductivity contributions is shown in the SI.

Figure 2 and Figure 3 show this fit of the Cole-Cole contribution to the sodium and proton phase data: the fits are represented by the solid lines. In the fitting procedure, the measurement series of the GHz-setup on the Nafion at 44% RH are combined with the measurement series of the THz-setup on the 50% RH Nafion. The measurement series of the GHz-setup on the 75% RH Nafion are combined with linearly interpolated values determined using the 50% RH and the 99% RH measurement series of the THz-setup.

The values of the reorientation time, τ, extracted from the fitting procedure are given in Table 1. At low water contents (at λ_{tot} = 0.5 for sodium terminated Nafion and λ_{tot} = 1 for protonated Nafion) the time constants could not be sufficiently well determined (Not Determined, ND) because the water signal is too weak. We observe that the reorientation time of the water molecules strongly depends on the water content. At low values of λ_{tot}, up to 4.5 for sodium terminated Nafion and up to 8.5 for protonated Nafion (at 44% and 75% RH), the reorientation time is tens of picoseconds, i.e. much larger than the Debye reorientation time of bulk liquid water at 300 K, τ_D, which

is 8.32 ps[18]. At the highest water contents, at λ_{tot} = 9 for sodium terminated Nafion and λ_{tot} = 12 for protonated Nafion (at 99% RH), the reorientation time of the water molecules is roughly equal to this Debye time. This shows that the water molecules are hindered in their rotational mobility at low values of λ_{tot}. This result is in agreement with previous studies that also show a slow-down of the water rotation in Nafion with decreasing λ_{tot}[19–21].

The reorientation of a water molecule in the bulk liquid proceeds via a transition state in which rotating a OH-group forms a bifurcated hydrogen donor bond with two water molecules[22]. An essential role in this rotation is played by the approach and drifting apart of the neighboring water molecules. When the H_2O concentration is low and a large fraction of the molecules are strongly bound to the sulfonate groups, the evolution to and from the transition state will be slowed down resulting in a much lower orientational mobility. At higher water contents the rotating OH-group is surrounded by water molecules making the reorientation time constant similar to that of bulk water. This behavior is found for both sodium terminated and protonated Nafion.

Table 1: Values of the fit parameters of the Cole-Cole model for sodium terminated and protonated Nafion at a range of water contents (λ_{tot}) and Relative Humidities (RH). Some values could not be determined (ND). For comparison the values for pure bulk water are given.

λ_{tot}		RH	τ [ps]		α		σ [S/m]	
Na	H		Na	H	Na	H	Na	H
0.5 ± 0.5	1.0 ± 0.5	00%	ND	ND	ND	ND	0.00 ± 0.01	0.02 ± 0.01
1.0 ± 0.5	4.0 ± 0.5	44%	45 ± 5	40 ± 5	0.67 ± 0.08	0.53 ± 0.07	0.04 ± 0.03	0.84 ± 0.05
4.5 ± 0.5	8.5 ± 0.5	75%	21 ± 5	22 ± 4	0.56 ± 0.07	0.51 ± 0.05	0.26 ± 0.01	2.39 ± 0.09
9.0 ± 0.5	12.0 ± 0.5	99%	10.0 ± 0.9	7.3 ± 0.8	0.43 ± 0.03	0.34 ± 0.03	0.93 ± 0.02	5.5 ± 0.1
Bulk water			8.32		0		0	

The values obtained for α from the fits are given in Table 1. We find that α decreases with increasing water content, in both the sodium terminated and the protonated Nafion. This means that the distribution of reorientation times becomes narrower at higher water contents, suggesting that the environment of the water molecules becomes more homogeneous with increasing λ_{tot}.

Table 1 gives the values for the conductivity, σ, both for sodium terminated and protonated Nafion. The latter are in good agreement with a previous study of Choi et al.[14] It is seen that the conductivity for protonated Nafion is much higher than for sodium terminated Nafion. In

bulk water, the molar conductivity $\sigma_{M,H,BW}$ of protons is $349.8 \cdot 10^{-4}$ S-m^2/mol, while the molar conductivity of sodium ions, $\sigma_{M,Na,BW}$, is $50.1 \cdot 10^{-4}$ S-m^2/mol[1]. Under the assumption that all ionic groups in the Nafion are dissociated at the highest hydration levels here achived (λ_{tot} = 9 for sodium terminated Nafion and λ_{tot} = 12 for protonated Nafion – see further discussion concerning ionic dissociation in connection to Eq. 6), the molar conductivity of the sodium ions and the protons in the Nafion membranes is found to be only $\sim$10% of the molar conductivities in bulk liquid water.

It is of interest to note that the conductivity of the protonated Nafion decreases more strongly with decreasing λ than for the sodium phase Nafion. This suggests that the conduction mechanism of the two cations in the Nafion are indeed distinctly different and that the effective mobility of the proton relies on a more extended hydration structure (thus being more strongly perturbed when the hydration level decreases), in line with the idea that protons are largely conducted via the Grotthuss mechanism.

We derived the number of rotationally mobile water molecules per Nafion polymer unit, $\lambda_{Cole-Cole}$, from the amplitude of the Cole-Cole mode using the following equation[23]:

$$\lambda_{Cole-Cole} = \frac{S_1}{S_{1,water}} \cdot \frac{c_{water} M_{Nafion}}{\rho_{Nafion}} \,. \tag{4}$$

Here, ρ_{Nafion} is the density of Nafion[8] (2.05 g/cm^3) and c_{water} is the molar concentration of water at 25 °C ($55.33 \cdot 10^{-3}$ mol/cm^3). Previous studies showed that the density, ρ_{Nafion}, is approximately constant over the whole range of possible degrees of hydration[8]. The number of rotationally mobile water molecules per Nafion sulfonate group as a function of the total water content, as obtained directly from our dielectric relaxation measurements, is represented by the blue lines in Figure 4.

Figure 4 shows that the number of rotationally mobile water molecules (i.e. those contributing to the dielectric relaxation), determined using the strength of the Cole-Cole mode, is smaller than the total water content determined by weighing the samples (λ_{tot}). This difference suggests that part of the water is not able to move freely and is therefore not contributing to the dielectric

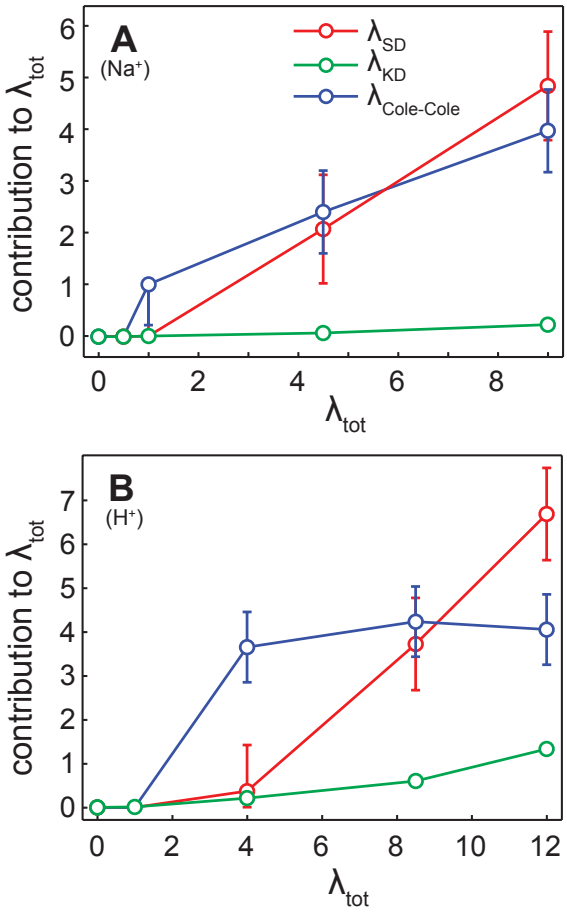

Figure 4: The number of static depolarized (SD), kinetic depolarized (KD) and rotationally mobile (Cole-Cole) water molecules per sulfonate group as a function of the total water content of the Nafion for (A) sodium terminated Nafion and (B) protonated Nafion. The contributions of the different types of water molecules are described in the text.

response. Two phenomena can account for this: kinetic and static depolarization.

Kinetic depolarization arises since water molecules that are close to ions that are moved by the EM wave are forced to reorient their dipoles in a direction opposite to this field, leading to a depolarization contribution. The strength of this kinetic depolarization is given by[24]:

$$\Delta_{KD}S_1 = \frac{2}{3} \cdot \frac{S_{1,water}}{S_{1,water} + \varepsilon_{\infty,water}} \cdot \frac{\tau_D}{\varepsilon_0}\sigma \ . \tag{5}$$

Using Eq. (4) with S_1 replaced by $\Delta_{KD}S_1$, the green lines in Figure 4 are calculated, representing λ_{KD}.

The second form of depolarization arises since cations can irrotationally bind water molecules, with the result that these water molecules no longer relax with respect to the external electric field[18]. This depolarization contribution is often denoted as static depolarization and is assumed to account for the remaining part of the difference between the rotationally mobile water molecules determined using the strength of the Cole-Cole mode and the total water content determined by weighing the samples.

The number of water molecules that are irrotationally bound to cations depends on two parameters: the number of free cations in the medium and the number of water molecules that are irrotationally bound per cation. In Nafion, the number of cations depends on the dissociation constant of the Nafion, i.e. the percentage of protons or sodium ions that has detached from the sulfonated side chain. Also the number of water molecules that are irrotationally bound per cation may vary. In bulk water, a proton can irrotationally bind up to four water molecules[23], as can a sodium cation[24–27].

The red lines in Figure 4 indicate the number of irrotationally bound water molecules (static depolarized water molecules) per Nafion side chain, λ_{SD}. This number varies with the total water content. At low values of λ_{tot}, the number of irrotationally bound water molecules per Nafion side chain is lower than four. This is probably due to the fact that at these low water contents, not all ion pairs (SO_3^- and H^+/Na^+) are dissociated, which is in agreement with earlier research where the deprotonation of Nafion has been investigated using quantum chemical modeling of the infrared

spectra[13] and molecular orbital calculations[11]. These studies have shown a deprotonation of the perfluorosulfonic side-chains when λ_{tot} reaches a value of 3 to 4. This increase in dissociation is also visible as a strong increase in the number of static depolarized water molecules in the 44 - 75% RH range (λ_{tot} = 1 to 4.5 for sodium terminated Nafion and λ_{tot} = 4 to 8.5 for protonated Nafion).

At the highest values of λ_{tot} the number of static depolarized water molecules per Nafion side chain is larger than 4. Even if all ion pairs have dissociated at this value of λ_{tot}, which is the case according to previous research[11,13], this means that the number of water molecules that are irrotationally bound per cation is larger in Nafion than in bulk water. This might be due to the existence of solvent separated ion pairs consisting of the anionic side chains and the cationic protons or sodium ions. This interaction may lead to binding of additional water molecules that show an extremely low orientational mobility.

Using the conductivity of the Nafion samples and assuming that all the ion pairs are dissociated at 99% RH (λ_{tot} = 9 for sodium terminated Nafion and λ_{tot} = 12 for protonated Nafion), the molar conductivity of the cations can be calculated. For sodium terminated Nafion this is done using:

$$\sigma_{M,Na,Nafion} = \frac{\sigma_{Na} M_{Nafion}}{\rho_{Nafion}} \tag{6}$$

where σ_{Na} the measured conductivity of the sodium terminated Nafion. The same expression can be used to calculate the molar conductivity of protons in the protonated Nafion.

We find values of the molar conductivity of protonated Nafion of $34 \pm 3 \cdot 10^{-4}$ S-m^2/mol and sodium terminated Nafion of $4.3 \pm 0.5 \cdot 10^{-4}$ S-m^2/mol at 99% RH. Comparing these results with the molar conductivity of protons ($349.8 \cdot 10^{-4}$ S-m^2/mol) and sodium ions ($50.10 \cdot 10^{-4}$ S-m^2/mol) in bulk water it can be seen that the Nafion environment induces a drastic reduction of the molar conductivity of the cations, resulting in values of only $\sim$10% of the molar conductivity of bulk water.

Conclusions

Hydrated proton and sodium phase Nafion has been investigated by measuring the complex permittivity in the 1.5–20 GHz and 0.7–1.5 THz frequency range. For the GHz frequency range we used an open probe coaxial reflectometric setup and for the THz frequency range we employed a time-domain THz transmission setup. We measured permittivity curves of Nafion membranes with a water content ranging from 1 to 12 water molecules per Nafion sulfonate group.

We fitted the measured permittivity curves with a Cole-Cole relaxation mode plus a conductivity term. At low water content ($\lambda_{tot} = 1$ for sodium terminated Nafion and $\lambda_{tot} = 4$ for protonated Nafion) we find a value of the reorientation time, τ, of 45 ± 5 picoseconds for sodium terminated Nafion and 40 ± 5 picoseconds for protonated Nafion. At the highest values of λ_{tot} (9 for sodium terminated Nafion and 12 for protonated Nafion) we find 10.0 ± 0.9 ps and 7.3 ± 0.8 ps, respectively. At the same water contents, the time distribution parameter α ranges from 0.67 ± 0.08 (Na terminated Nafion) and 0.53 ± 0.07 (H terminated Nafion) to 0.43 ± 0.03 (Na) and 0.34 ± 0.03 (H), respectively. The conductivity at the lowest water contents is below the detection limit for both types of Nafion and increases to 0.93 ± 0.02 S/m for sodium terminated Nafion and 5.5 ± 0.1 S/m for protonated Nafion at the highest values of λ_{tot}.

The measured dielectric response only corresponds to part of the water molecules present in the Nafion membranes. The other water molecules are primarily irrotationaly bound to the cations, since kinetic depolarization is found to only account for a very small part of the missing water response. At the highest values of λ_{tot}, the irrotationally bound water fraction exceeds 4 water molecules per cation (the number of rotational immobilized water molecules per cation in bulk water), which might be due to the formation of solvent separated ion pairs between the sulfonate groups of the Nafion side chains and the cations.

Even at the highest water content ($\lambda_{tot} = 9$ for sodium terminated Nafion and $\lambda_{tot} = 12$ for protonated Nafion), the molar conductivity of the sodium ions and the protons in the Nafion membranes is found to be only $\sim$10% of the molar conductivities in bulk liquid water.

Finally, we have found that the conductivity of the protonated Nafion decreases more strongly

upon a decrease of the hydration level than the conductivity of the Nafion containing sodium ions. This is a consequence of that the structural diffusion of the hydrated proton requires a more extended hydration shell to be fully efficient whereas the mass transport of the sodium ion is less sensitive to the extent of its hydration sphere.

Acknowledgements

This work is part of the research program of the Foundation for Fundamental Research on Matter (FOM), which is part of the Netherlands Organisation for Scientific Research (NWO). The authors would like to acknowledge technical support by H. Schoenmaker and H.-J. Boluijt. Furthermore, Yves Rezus is gratefully acknowledged for giving many valuable comments and suggestions to drafts of this manuscript. W.E. would like to thank prof. dr. J.I. Dijkhuis of the Utrecht University for many valuable discussions. J.H. thanks the Deutsche Forschungsgemeinschaft (DFG) for funding through the award of a research fellowship. N.O. gratefully acknowledges the European Commission (FP7) for funding through the award of a Marie Curie fellowship.

References

(1) Marcus, Y. *Ion properties*; CRC, 1997.

(2) Agmon, N. The Grotthuss Mechanism. *Chem. Phys. Lett.* **1995**, *244*, 456 – 462.

(3) Marx, D. Proton Transfer 200 Years after von Grotthuss: Insights from Ab Initio Simulations. *Chem. Phys. Chem.* **2006**, *7*, 1848–1870.

(4) Chandra, A.; Tuckerman, M.; Marx, D. Connecting Solvation Shell Structure to Proton Transport Kinetics in Hydrogen-Bonded Networks via Population Correlation Functions. *Phys. Rev. Lett.* **2007**, *99*, 145901.

(5) Cukierman, S.; Quigley, E. P.; Crumrine, D. S. Attenuation of Proton Currents by Methanol

in a Dioxolane-Linked Gramicidin A Channel in Different Lipid Bilayers. *Biophys. J.* **1997**, *73*, 2489 – 2502.

(6) Brewer, M. L.; Schmitt, U. W.; Voth, G. A. Molecular Dynamics Simulation of Proton Transport through the Influenza A Virus M2 Channel. *Biophys. J.* **2001**, *80*, 1691 – 1702.

(7) Schmidt-Rohr, K.; Chen, Q. Parallel Cylindrical Water Nanochannels in Nafion Fuel-Cell Membranes. *Nature* **2007**, *7*, 75 – 83.

(8) Zook, L. A.; Leddy, J. Density and Solubility of Nafion: Recast, Annealed, and Commercial Films. *Anal. Chem.* **1996**, *68*, 3793 – 3796.

(9) Elliott, J. A.; Wu, D.; Paddison, S. J.; Moore, R. B. A Unified Morphological Description of Nafion Membranes from SAXS and Mesoscale Simulations. *Soft Matter* **2011**, *7*, 6820 – 6827.

(10) Haubold, H.; Vad, T.; Jungbluth, H.; Hiller, P. Nano Structure of NAFION: A SAXS Study. *Electrochim. Acta* **2001**, *46*, 1559 – 1563.

(11) Paddison, S. J.; Elliott, J. A. Selective Hydration of the 'Short-Side-Chain' Perfluorosulfonic Acid Membrane. An ONIOM Study. *Solid State Ionics* **2007**, *178*, 561 – 567.

(12) Anantaraman, A.; Gardner, C. Studies on Ion-Exchange Membranes. I. Effect of Humidity on the Conductivity of Nafion. *J. Electroanal. Chem.* **1996**, *414*, 115 – 120.

(13) Laflamme, P.; Beaudoin, A.; Chapaton, T.; Spino, C.; Soldera, A. Molecular Modeling Assisted Design of New Monomers Utilized in Fuel Cell Proton Exchange Membranes. *J. Membr. Sci.* **2012**, *401*, 56 – 60.

(14) Choi, P.; Jalani, N. H.; Datta, R. Thermodynamics and Proton Transport in Nafion II. Proton Diffusion Mechanisms and Conductivity. *J. Electrochem. Soc.* **2005**, *152*, E123 – E130.

(15) Renou, J.; Bonnet, M.; Bielicki, G.; Rochdi, A.; Gatellier, P. NMR study of Collagen-Water Interactions. *Structures Tissulaires et Interactions Moleculaires,* **1994**, *1*, 1615 – 1626.

(16) Zawodzinski, T. A.; Derouin, C.; Radzinski, S.; Sherman, R. J.; Smith, V. T.; Springer, T. E.; Gottesfeld, S. Water Uptake by and Transport Through Nafion 117 Membranes. *J. Electrochem. Soc.* **1993**, *140*, 1041 – 1047.

(17) Material Safety Data Sheet, Sigma-Aldrich, Nafion Perfluorinated Membrane.

(18) Buchner, R.; Barthel, J.; Stauber, J. The Dielectric Relaxation of Water Between 0°C and 35°C. *Chem. Phys. Lett.* **1999**, *306*, 57–63.

(19) Petersen, M.; Hatt, A.; Voth, G. Orientational Dynamics of Water in the Nafion Polymer Electrolyte Membrane and Its Relationship to Proton Transport. *J. Phys. Chem. B* **2008**, *112*, 7754–7761.

(20) Lu, Z.; Polizos, G.; Macdonald, D.; Manias, E. State of Water in Perfluorosulfonic Ionomer (Nafion 117) Proton Exchange Membranes. *J. Electrochem. Soc.* **2008**, *155*, B163–B171.

(21) Moilanen, D.; Piletic, I.; Fayer, M. Water Dynamics in Nafion Fuel Cell Membranes: The Effects of Confinement and Structural Changes on the Hydrogen Bond Network. *J. Phys. Chem. C* **2007**, *111*, 8884–8891.

(22) Laage, D.; Hynes, J. A Molecular Jump Mechanism of Water Reorientation. *Science* **2006**, *311*, 832–835.

(23) Tielrooij, K.-J.; Timmer, R.; Bakker, H.; Bonn, M. Structure Dynamics of the Proton in Liquid Water Probed with Terahertz Time-Domain Spectroscopy *Phys. Rev. Lett.* **2009**, *102*, 198303(1–4).

(24) Buchner, R.; Hefter, G. T.; May, P. M. Dielectric Relaxation of Aqueous NaCl Solutions *J. Phys. Chem. A* **1999**, *103*, 1 – 9.

(25) Ahmad, N.; Day, M. The Solvation Number of the Sodium Ion. *J. Inorg. Nucl. Chem.* **1978**, *40*, 1383 – 1385.

(26) Barnett, R.; Landman, U. Hydration of Sodium in Water Clusters. *Phys. Rev. Lett.* **1993**, *70*, 1775 – 1778.

(27) White, J. A.; Schwegler, E.; Galli, G.; Gygi, F. The Solvation of Na^+ in Water: First-Principles Simulations. *J. Chem. Phys.* **2000**, *113*, 4668 – 4673.

(28) Buchner, R.; Barthel, J. Dielectric Relaxation in Solutions. *Annu. Rep. Prog. Chem.* **2001**, *97*, 349 – 382

.

Supplementary Information for "On the Orientational Mobility of Water Molecules in Proton and Sodium Terminated Nafion Membranes"

W. Ensing,[†] J. Hunger,[†,‡] N. Ottosson,[*,†] and H.J. Bakker[†]

FOM Institute AMOLF, Science Park 104, 1098 XG Amsterdam, The Netherlands

E-mail: ottosson@amolf.nl

[*]To whom correspondence should be addressed

[†]FOM Institute AMOLF, Science Park 104, 1098 XG Amsterdam, The Netherlands

[‡]Present: Molecular Spectroscopy Department, Max Planck Institute for Polymer Research, Ackermannweg 10, 55128 Mainz, Germany

GHz Frequency Domain Reflectometer

To measure complex permittivity spectra at frequencies ranging from 1.5–20 GHz we use a frequency domain reflectometer based on a Vector Network Analyser (VNA, ZVA67 Rohde & Schwarz GmbH & Co KG, Germany). The VNA is connected to a home-built open-ended coaxial probe (Figure 1) using two phase stable, 1.85 mm connector, 0.6 m long coaxial cables (ZV-Z96 Rohde & Schwarz).

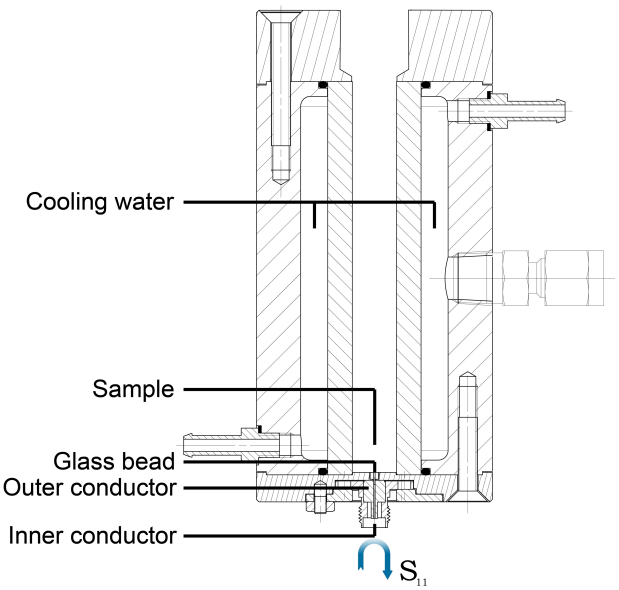

Figure 1: Schematic cross-section of the home-built probe head of the GHz-setup.

The VNA measures the effective scattering parameter, $\hat{S}_{11}(\omega)$, resulting from the reflection of the signal on the probe head-sample interface. For our present setup the scattering parameters are dominated by the impedance step at the coaxial cable - sample interface. For a single impedance step the scattering parameter is related to the normalized (with respect to the $50\,\Omega$ impedance of the coaxial cable) impedance, $\hat{Y}(\omega)$, by:[1]

$$\hat{S}_{11}(\omega) = \frac{1-\hat{Y}(\omega)}{1+\hat{Y}(\omega)}\,. \tag{1}$$

The dimensions of the home-built probe head (Figure 1) are such that it is impedance matched with the ZV-Z96 coaxial cable. A circular flange terminates the outer conductor. A glass bead is

located in the flange at the end of the inner conductor to prevent liquid samples from entering the coaxial cable. The contact area with the sample consists of a circular plane with a 9.1 mm diameter. This suffices to ensure that the EM fields are, to a good approximation, zero at the boundaries, ensuring that the assumption of an infinite half sphere holds.[2] The normalized impedance of the sample, $\hat{Y}(\omega)$, can be computed for this open-ended probe geometry, assuming only the principal mode to be present in the coaxial cable. The equation for the normalized impedance found under these conditions by Blackham is:[2]

$$\hat{Y}(\omega) = \frac{\hat{k}_m^2(\omega)}{\pi \hat{k}_c(\omega) \ln(D/d)} \times \left[i \left(\frac{I_1}{0!} - \frac{\hat{k}_m^2(\omega) I_3}{2!} + \frac{\hat{k}_m^4(\omega) I_5}{4!} - \dots \right) + \right.$$

$$\left. \left(\frac{\hat{k}_m(\omega) I_2}{1!} - \frac{\hat{k}_m^3(\omega) I_4}{3!} + \frac{\hat{k}_m^5(\omega) I_6}{5!} - \dots \right) \right] \tag{2}$$

Here, $\hat{k}_m(\omega) = \omega \sqrt{\hat{\varepsilon}(\omega) \varepsilon_0 \mu_0}$ is the propagation constant of the sample at frequency ω, μ_0 is the vacuum permeability, $\hat{k}_c(\omega) = \omega \sqrt{\hat{\varepsilon}_c \varepsilon_0 \mu_0}$ is the propagation constant in the probe head, D is the inside diameter of the outer conductor, and d is the outside diameter of the inner conductor. The elements I_n, $n \in [1, 2, \dots 40]$, are coefficients resulting from the Taylor expansion of the normalized impedance and depend on the geometric configuration of the setup. All coefficients I_n were computed via numerical integration of Eq. (3):[2]

$$I_n' = \int_d^D \int_d^D \int_0^\pi \left(\sqrt{r^2 + r'^2 - 2rr' \cos(\theta)} \right)^{n-2} \cos(\theta) d\theta \; dr \; dr' \tag{3}$$

The thus obtained coefficients were empirically refined following the route outlined in Ref. 2. This optimization was performed by fitting calculated $|S_{11}|$ values according to Eq. (2) to the modulus of measured scattering parameters for a series of reference liquids, while the cable losses were taken to be independent of the sample (i.e. water,[3] aqueous solutions of NaCl,[4] *N*,*N*-dimethylacetamide,[5] propylene carbonate,[6], methanol,[7] ethanol,[7] and 2-propanol[7]).

As the VNA provides only relative measurements of the reflected wave with respect to an arbitrary reference wave the instrumentation needs to be calibrated. This calibration was performed

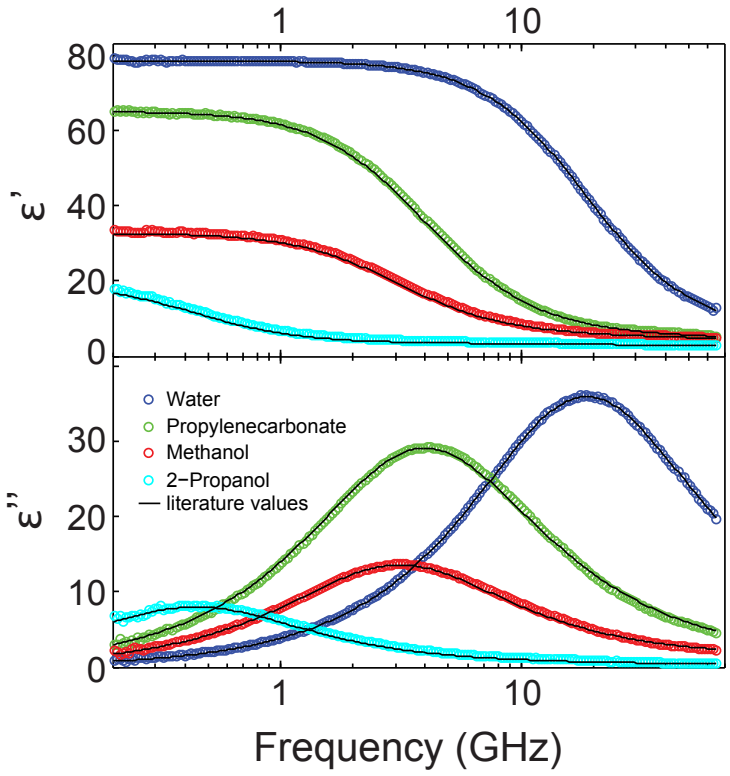

Figure 2: Dielectric permittivity spectra for several reference liquids ranging from samples with high (water) to low (2-propanol) permittivities. Symbols correspond to experimental data recorded at 25 °C with the present experimental setup. Solid lines correspond to literature spectra.[3,6,7]

prior to each measurement series using an one-port, three-term error model,[1,2] which relates the relative measured scattering parameters, $S_{11}^{\mathrm{m}}(\omega)$, to the actual scattering parameters at the sample-coaxial probe interface, $S_{11}^{\mathrm{a}}(\omega)$:

$$S_{11}^{\mathrm{m}}(\omega) = e_{\mathrm{d}}(\omega) + \frac{e_{\mathrm{r}}(\omega) S_{11}^{\mathrm{a}}(\omega)}{1 - e_{\mathrm{s}}(\omega) S_{11}^{\mathrm{a}}(\omega)} \tag{4}$$

The errors of directivity, $e_{\mathrm{d}}(\omega)$, frequency response, $e_{\mathrm{r}}(\omega)$, and source match, $e_{\mathrm{s}}(\omega)$, were determined at each single frequency by performing three reflection measurements for water, air, and a gold foil (short).

For each sample measurement the reflection coefficient at the sample - coaxial probe interface, S_{11}^{a}, was calculated from the measured value of S_{11}^{m} using eq. Eq. (4). The values of $\hat{\varepsilon}(\omega)$ of the sample were subsequently determined with Eq. (1) and Eq. (2) using a nonlinear optimization based on a simplex algorithm.

The sample, which is positioned on top of the glass bead, is more than 0.5 cm thick and kept in a temperature-controlled jacket at 25 °C. As can be seen in Figure 2, the spectra recorded with our present setup are in excellent agreement with spectra reported in literature and the accuracy of the present experiment is estimated to be better than 2 %.

THz dielectric relaxation

Figure 3A shows the time-domain terahertz (THz) spectroscopy setup. We split ∼75 milliwatts of the output of an 800 nm, 110 fs, 1 kHz pulsed Ti:sapphire laser into two branches to generate and to detect the THz pulses with a spectrum covering 0.7–1.5 THz. The single-cycle THz-pulse is generated via optical rectification in a nonlinear ZnTe crystal. The THz pulse is transmitted through the sample and focused on a second ZnTe detection crystal. The sample is held between two PCTFE (Polychlorotrifluoroethylene) windows separated by a teflon spacer yielding a sealed chamber, see Figure 3B. The sample cell has two compartments, which are alternately put into the focus of the THz beam. One compartment of the cell contains the sample, the other compartment

is an empty reference used to correct for laser drifts.

The 800 nm pulse used for the detection is passed through a delay line and is spatially overlapped with the THz-pulse on the ZnTe detection crystal. The temporal overlap with the THz-pulse is controlled using a delay line. At the detection crystal, the polarization ellipticity of the initially linearly polarized detection pulse is changed due to the induced birefringence in the ZnTe under influence of the electric field of the THz-pulse. This change in ellipticity is detected using a quarter wave plate, a polarizing beamsplitter, and a differential detector.[8] The generation beam is chopped at 500 Hz to allow for background subtraction. A gated integrator (Stanford Research Systems SR250) is used to record both the THz pulses that are transmitted through the empty cuvette and the THz pulses that are transmitted through the Nafion filled cuvette. An air measurement is done by removing the rotating sample holder from the setup. The thickness of the cuvette windows is 1.980 mm and the air filled chamber has a length of 0.180 mm.

The ratio of the frequency components of the pulse travelling through the sample and those of the pulse travelling though an empty cuvette, $E_{sam}(\omega)/E_{cuv}(\omega)$, is given in terms of the propagation coefficients, p_i, transmission coefficients, t_{ij}, and reflection coefficients, r_{ij}, as:[9]

$$\frac{E_{sam}(\omega)}{E_{cuv}(\omega)} = \frac{t_{23}p_3t_{34}(1+r'_{23}r'_{34}{p'_3}^2)}{t'_{23}p'_3t'_{34}(1+r_{23}r_{34}{p_3}^2)} \tag{5}$$

The index 3 represents air, the index in a primed coefficient and Nafion in a non-primed coefficient, the indices 2 and 4 represent the window material (PCTFE), see Figure 3B. The refractive index of the cuvette material is determined in a separate measurement in which the transmission of the empty cuvette is compared with that of air. Hence, all variables are known except the complex refractive index of the Nafion, $\hat{n}(\omega)$. The complex refractive index of the hydrated Nafion is obtained by fitting the measured ratio of the frequency components of the THz pulse transmitted through the Nafion filled cuvette and the empty cuvette to Eq. (5). The permittivity, $\hat{\varepsilon}(\omega)$, can be determined by the relation $\hat{\varepsilon}(\omega) = \hat{n}(\omega)^2$.

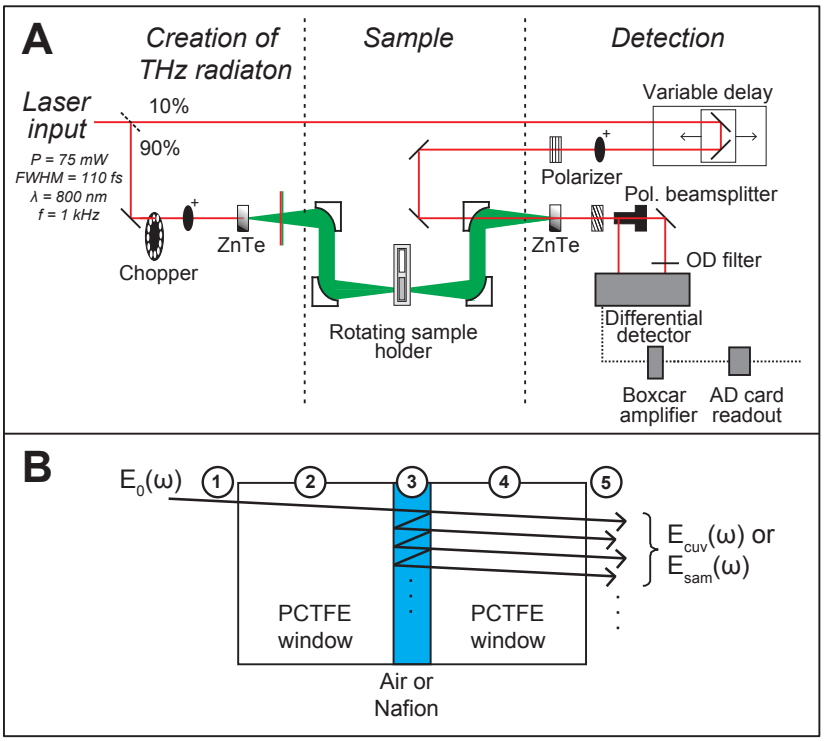

Figure 3: (A) Schematic outline of the THz-setup and (B) a graphical representation of a THz-pulse traveling though an air/Nafion-filled cuvette. The ratios of the frequency components of the THz-pulses transmitted through air and those transmitted through Nafion are described by Eq. (5). These ratios are used to determine the permittivity.

Decomposition of measured spectra into dielectric relaxation and conductivity contributions

Figures 2 and 3 of the main article presented the dielectric relaxation of water dipoles in the sodium phase and proton phase Nafion membranes, respectively, after subtraction of the conductivity response. However, the measured dielectric loss ε''' is dominated by the conductivity loss term $\sigma/\varepsilon_0\omega$ (where σ is the conductivity, ε_0 is vacuum permittivity and ω is the angular frequency of the external electric field) especially at higher hydration levels. Figure 4 gives the measured raw data for the proton phase Nafion. The top panel shows the real part which is not affected by the ionic conductivity (thus being identical to the top panel given in Fig. 3 in the main article). The middle part represents the total fit to ε'' given by Eq. 3 in the main text, whereas the bottom part shows the decomposition of ε'' into conductivity and dielectric relaxation contributions, i.e. given by the first and second term in the fit model, respectively.

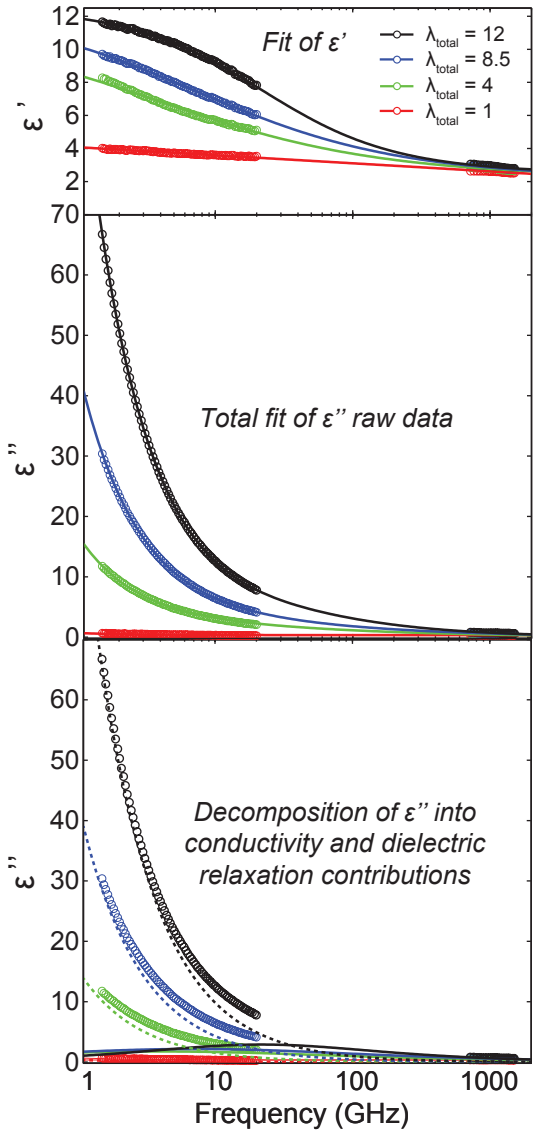

Figure 4: Raw dielectric spectra of protonated Nafion at various hydration levels. ε' in the top figure gives the in-phase polarization of the sample and the middle and bottom parts show ε'', i.e. the imaginary part the loss (dissipation) in the sample before subtraction of the conductivity contribution (See Eq. 3 in the main text). The middle figure shows the total fit to the imaginary data whereas the bottom figure shows the fit decomposed into the conductivity response (dashed lines, dominating a low frequencies) and Cole-Cole dielectric relaxation modes (solid lines).

References

(1) Golio, J. *The RF and microwave handbook*; CRC PressI Llc, 2001.

(2) Blackham, D. V.; Pollard, R. D. An Improved Technique for Permittivity Measurements Using a Coaxial Probe. *IEEE Trans. Instrum. Meas.* **1997**, *46*, 1093 – 1099.

(3) Ellison, W. J. Permittivity of Pure Water, at Standard Atmospheric Pressure, over the Frequency Range 0–25 THz and the Temperature Range 0–100 °C. *J. Phys. Chem. Ref. Data* **2007**, *36*, 1 – 18.

(4) Buchner, R.; Hefter, G. T.; May, P. M. Dielectric Relaxation of Aqueous NaCl Solutions. *J. Phys. Chem. A* **1999**, *103*, 1 – 9.

(5) Barthel, J.; Buchner, R.; Wurm, B. The Dynamics of Liquid Formamide, N-methylformamide, N,N-dimethylformamide, and N,N-dimethylacetamide. A Dielectric Relaxation Study. *J. Mol. Liq.* **2002**, *98 – 99*, 51 – 69.

(6) Barthel, J.; Buchner, R.; Hölzl, C. G.; Münsterer, M. Dynamics of Benzonitrile, Propylene Carbonate, and Butylene Carbonate: The Influence of Molecular Shape and Flexibility on the Dielectric Relaxation Behaviour of Dipolar Aprotic Liquids. *Z. Physikal. Chem.* **2000**, *214*, 1213 – 1231.

(7) Barthel, J.; Bachhuber, K.; Buchner, R.; Hetzenauer, H. Dielectric Spectra of Some Common Solvents in the Microwave Region. Water and Lower Alcohols. *Chem. Phys. Lett.* **1990**, *165*, 369 – 373.

(8) Tielrooij, K.-J.; Van Der Post, S.; Hunger, J.; Bonn, M.; Bakker, H. Anisotropic Water Reorientation around Ions. *J. Phys. Chem. B* **2011**, *115*, 12638–12647.

(9) Griffiths, D. In *Introduction to Electrodynamics (Chapter 9)*; Kindersley, D., Ed.; Pearson Education, 2007.